Journal of ELECTRICAL ENGINEERING, VOL 73(2022), NO6, 378–386

sciendo

PAPERS

Single channel convolutive blind source separation for LFM radar signals

Pengfei Xu, Yinjie Jia*, Xinnian Guo[1]

We propose a single channel blind source separation algorithm for convolutively mixed linear frequency modulation (LFM) signals based on smoothed Wigner-Ville distribution (SWVD) time-frequency analysis, Canny edge detection, and Hough transform detection. First, the SWVD time-frequency analysis diagram is obtained as an image based on the LFM time-frequency characteristics. Second, Canny edge detection is performed on the image. Then, Hough transform is used to detect the characteristic parameters of the linear signal. Finally, the source signal is recovered. The simulation results show that the algorithm is effective for single channel detection and extraction of convolutively mixed LFM signals.

K e y w o r d s: convolutive blind source separation, single channel, time-frequency distributions, smoothed Wigner-Ville distribution, Canny edge detection, Hough transform, line detection, linear frequency modulation signal

1 Introduction

Most convolutively mixed blind source separation algorithms are mainly used in the case of overdetermined or well-posed blind source separation. These algorithms are not applicable to underdetermined blind source separation, wherein the number of mixed signals is less than the number of source signals. An extreme case in underdetermined blind source separation is single channel blind source separation (SCBSS), which refers to the process of using a single receiving sensor to receive the observation signal and using only this observation signal to recover each source signal; this process poses an ill-conditioned problem [1], which is difficult to solve. SCBSS under a convolutively mixed model is a challenging topic. A linear frequency modulation (LFM) signal is one of the signal waveforms often used in modern high-performance radar systems. Compared with other pulse compression signals, LFM signals are easy to be generated by digital technology, which is a relatively well-established technology that is widely used in engineering. In this study, the LFM signal is taken as an example to study convolutively mixed SCBSS based on the time-frequency domain.

Compared with underdetermined blind source separation with more than two observation signals, the processing method of single-observation-signal blind source separation has changed substantially, because the mathematical model based on matrix representation and the corresponding analysis method is no longer applicable. Due to the lack of information available for direct use in SCBSS, it is necessary to fully exploit and utilize the different potential characteristics of signals, including statistical, time domain, frequency domain, and time-frequency domain characteristics. At present, the theoretical research and development of using these characteristics of signals to solve the SCBSS problem is not yet developed. Compared with adaptive or overdetermined blind source separation, SCBSS requires less hardware and incurs lower system cost and, thus, has important, wide application prospects and practical research significance. Suppose m source signals are transmitted through a wireless channel and converge to a receiving sensor. The schematic diagram of SCBSS is shown in Fig. 1.

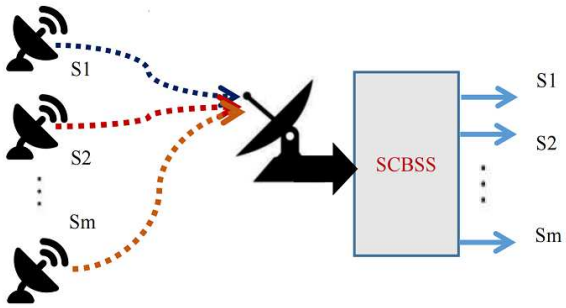

Fig. 1. Schematic diagram of single channel blind source separation

To ensure the uniqueness of the source signal separated from the single channel mixed signal, the separability of the single channel mixed signal is crucial [2]. For solving the problem of blind source separation, it is important to determine how to mine and utilize the potential prior knowledge of the problem. In essence, the current SCBSS algorithms are based on the difference between signals. Signal analysis is far more than that in time, frequency, S, and Z domains. A domain is a very broad mathematical concept; any kind of transformation can be understood as a mapping from one domain to another. Signals in different domains can reflect different characteristics. In one domain, the signal may appear disorganized,

[1] School of Information Engineering, Suqian University, Suqian, Jiangsu 223800, China, * Corresponding author jiayinjie@squ.edu.cn

https://doi.org/10.2478/jee-2022-0052, Print (till 2015) ISSN 1335-3632, On-line ISSN 1339-309X

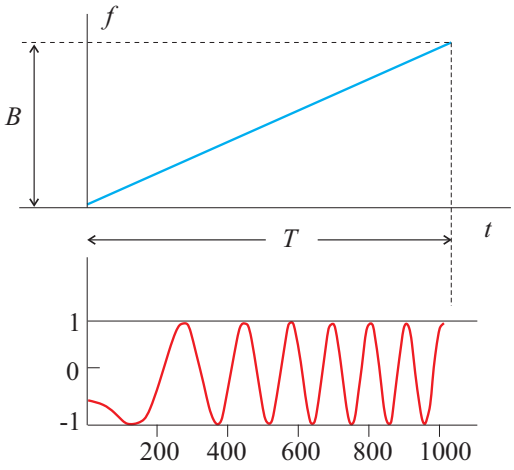

Fig. 2. Time-frequency domain and time domain waveforms of up-chirp 1 ($K > 0$)

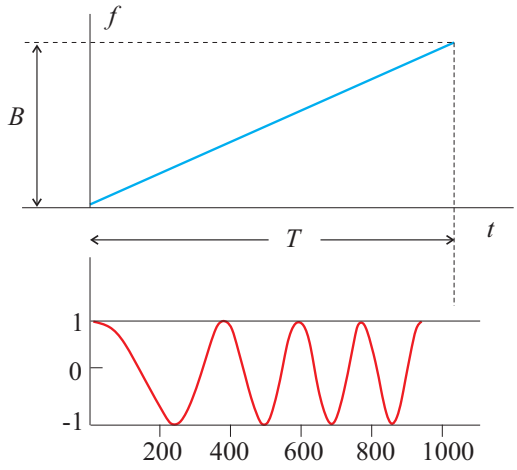

Fig. 3. Time-frequency domain and time domain waveforms of up-chirp 2 ($K > 0$)

whereas in another it may be regular, so domain transformation clearly shows some characteristics of the signal. Therefore, blind source separation can be realized as long as there are sufficient differences in domains such as time domain, frequency domain, time-frequency domain, or other transform domains. For some special signals, we can use their characteristics to develop a new blind source separation algorithm. The LFM signal is a typical non-stationary spread-spectrum signal waveform widely used in modern radar systems. It has a low probability of interception [3]. Its carrier frequency changes linearly in one cycle of the wide frequency band of the radiofrequency pulse signal, because of which the bandwidth of the signal is also broad. The LFM signal occupies much more bandwidth than information bandwidth, so it is also a spread spectrum modulation technology. The LFM signal is also called the chirp spread spectrum (CSS) signal because its bandwidth is within the audible range [4]. It is widely used in communication, radar, sonar, biomedical, and seismic exploration systems. Many natural phenomena can also use the chirp signal as the signal model [5]. Modern electronic reconnaissance systems often use the time-frequency analysis technology to detect and analyze such time-varying signals.

In this study, the LFM signal is taken as an example to introduce a convolutively mixed LFM signal blind source separation algorithm based on smoothed Wigner-Ville distribution (SWVD) time-frequency analysis [6], Canny edge detection [7], and Hough transform detection [8].

2 Methodology

2.1 Convolutively mixed LFM signals

The single LFM or chirp signal is mathematically expressed as follows

$$s(t) = \text{rect}(t/T)e^{j2\pi\left(f_c t + \frac{K}{2}t^2\right)}. \tag{1}$$

where f_c is the carrier frequency and $\text{rect}(t/T)$ is the rectangular signal.

$$\text{rect}(t * T) = \begin{cases} 1, & |t/T| \le 1, \\ 0, & \text{elsewise.} \end{cases} \tag{2}$$

$K = B/T$ is the frequency modulation slope, so the instantaneous frequency of the signal is $f_c + Kt$, $(0 \le t \le T)$.

The time-frequency domain and time domain waveforms of two LFM signals with different slopes are shown in Fig. 2 and Fig. 3.

These figures indicate that if the time-frequency analysis method is used to analyze the LFM signal, taking time and frequency as the two coordinate axes, the time-frequency distribution of the signal is a straight line. The up-chirp signal in equation (1) is rewritten as

$$s(t) = S(t)e^{j2\pi f_c t}, \tag{3}$$

where $S(t)$ is the complex envelope of signal $s(t)$, given by

$$S(t) = \text{rect}(t/T)e^{j\pi K t^2}. \tag{4}$$

According to the property of the Fourier transform, $s(t)$ and $S(t)$ have the same amplitude frequency characteristics. Therefore, only $s(t)$ needs to be considered in MATLAB simulation.

After multiple LFM signals propagate through multiple paths, the signals received by the sensors are convolutively mixed signals. At this time, the received signal is the sum of several LFM signals with different delays, and the attenuation of signal amplitude does not affect its time-frequency distribution characteristics.

For the convenience of discussion, it is assumed that two LFM signals $S_1(n)$ and $S_2(n)$ are transmitted to receiver $X_1(n)$ through two different paths. The ideal time-frequency distribution of $X_1(n)$ is shown in Fig. 4.

$$X_1(n) = a_{11}S_1(n) + a_{12}S_1(n - \tau_1) + a_{21}S_2(n) + a_{22}S_2(n - \tau_2). \tag{5}$$

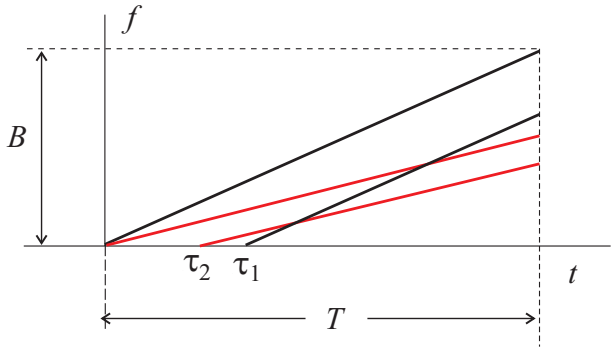

Fig. 4. Ideal time-frequency distribution of signal X_1

Figure 4 shows two groups of parallel lines in the time-frequency distribution diagram of the mixed signal $X_1(n)$ during the observation time T : one is the red line passing through the origin and the red line with delay τ_2, and the other is the black line passing through the origin and the black line with delay τ_2. The channel mixing coefficients a_{11}, a_{12}, a_{21}, and a_{22} have no effect on the time-frequency distribution diagram of the mixed signals. The figure also indicates that the time delay and signal amplitude (after energy fading) of the LFM source signal barely affect the shape of the time-frequency distribution of the source signals. We can judge the number of source signals according to the number of groups of parallel lines and thereby estimate some channel parameters such as the delay of each source signal.

2.2 SWVD time-frequency distribution

For multiple signal components with time-frequency overlapping, the instantaneous frequencies of each signal component may be extremely close owing to their overlapping spectrum, so the selected time-frequency distribution must have good resolution. At the same time, multiple signal components result in a large number of cross terms, which require the selected time-frequency distribution to have good cross-term suppression ability. These two are important problems of time-frequency distribution: resolution (or time-frequency aggregation) and cross-term suppression. An ideal time-frequency distribution should not only have high resolution in the time-frequency domain but also accurately reflect the instantaneous frequency of the signal.

The imaging effect of the time-frequency analysis method in Fig. 4 largely depends on the performance of the time-frequency distribution function. Time-frequency distributions are commonly obtained by short-time Fourier transform (STFT) [9], Wigner-Ville distribution (WVD) [13], and SWVD [6], among others. Considering the window function, the time-frequency resolution of STFT is related to the size of the window, so it is usually necessary to make a compromise between time resolution and frequency resolution.

WVD has the highest time-frequency resolution for the LFM signal, but it has more serious cross-term interference [10]. By contrast, compared with WVD, SWVD can suppress cross-term interference better, but its time-frequency resolution is lower.

The WVD expression of signal $S(t)$ is as follows [11]

$$W_{\mathrm{WVD}} = \int_{-\infty}^{\infty} S(t) + \frac{\tau}{2}) S^*(t - \frac{\tau}{2}) e^{-j2\pi f_d} \mathrm{d}\tau, \quad (6)$$

where t is the time, f_d is the frequency, and $S(t)$ is the sum of two signals with frequencies f_{d1} and f_{d2}. The expressions of WVD signal terms and cross terms are given in [11] as follows

$$P_{\mathrm{WVDauto}}(t, f_d) = \delta(f_d - f_{\mathrm{d1}}) + (f_d - f_{\mathrm{d2}}), \quad (7)$$

$$P_{\mathrm{WVDcross}}(t, f_d) = 2\delta\big(f_d - \tfrac{f_{\mathrm{d1}} + f_{\mathrm{d2}}}{2}\big) \cos[2\pi(f_{\mathrm{d1}} - f_{\mathrm{d2}})t]. \quad (8)$$

Equation (8) indicates that only the cross terms in WVD may have negative values. A two-dimensional smoothing window function $F(t, f_{\mathrm{d}})$ is constructed in the time-frequency domain and the SWVD of signal $S(t)$ can be formed by the low-pass filtering of the WVD of signal $S(t)$. The SWVD of signal $S(t)$ can be written as follows

$$W_{\mathrm{SWVD}}(t, f_d) = W_{\mathrm{WVD}}(t, f_d) * F(t, f_d). \quad (9)$$

The window width in the time and frequency domains can be set as required. As the low-pass filtering is performed, the time-frequency resolution of SWVD of the signal is low; however, it will not change the correct position of the signal term and can effectively suppress the cross-term interference. Therefore, SWVD is more suitable for the time-frequency analysis of multi-component signals. In this study, SWVD is selected to obtain the time-frequency diagram of convolutively mixed LFM signals.

2.3 Canny edge detection

Canny edge detection is used to improve the low time-frequency resolution of SWVD. The edge is generally a line composed of pixels in the image with sharp changes in light and shade. For edge detection, pixel-level binary classification is performed for the whole image. An edge point is indicated by white, while a non-edge point is indicated by black. Show these points and you will get an edge image. After binarization of the time-frequency image, we use the edge detection algorithm and Hough transform to detect the edge line. The commonly used edge detection algorithms are the Sobel operator, Laplacian operator, and Canny operator [7]. Edge extraction is also a kind of filtering, wherein different operators have different extraction effects. The Canny operator is not easily disturbed by noise and can detect weak edges; therefore, we select this edge detection method in this paper.

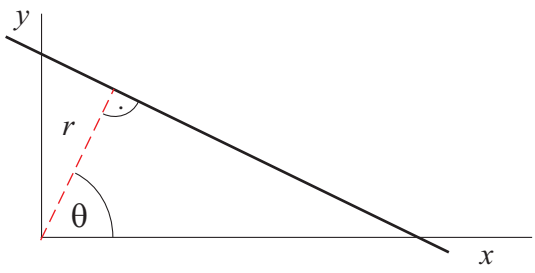

Fig. 5. Schematic diagram of the principle of Hough transform linear equation corresponding to these collinear points

Canny edge detection was proposed by John Canny in 1986. It is a multi-stage algorithm, comprising the following steps:

(1) Gaussian filtering

We know that the gradient operator can be used to enhance an image by enhancing the edge contour; that is, edges can be detected. However, the gradient operator is greatly affected by noise. Therefore, our first step is to eliminate the noise, because that is where the gray level changes greatly; thus, the noise can be easily recognized as a pseudo edge.

(2) Calculation of the image gradient

The image gradient is calculated to obtain the edge of the image, because the obvious gray level changes in the gradient correspond to edges. However, what we obtain in this step is all possible sets of edges, because the gray changes may or may not be an edge.

(3) Non-maximum suppression

In general, the gray changes are concentrated in certain edge points. In the gradient direction of the local range, the maximum gray changes are retained, while the others are eliminated. In this way, an edge with a multiple-pixel width is transformed into that with a single-pixel width. That is, a "fat edge" becomes a "thin edge".

(4) Double-threshold screening

After non-maximum suppression, there are still many possible edge points, so a double threshold, that is, low and high thresholds, is further set. If the gray level change is greater than the high threshold, the pixel is set as a strong edge pixel, and if it is lower than the low threshold, the pixel is rejected. The gray level change is between the low and high thresholds, the pixel is set as a weak edge. Further, the strong edge pixels in the field are retained, while the weak ones are eliminated. This step ensures that only the strong edge contour is retained. Some edges may not be closed, so we need to supplement the points between low and high to make the edge as closed as possible.

Overall, the multi-stage edge detection algorithm can be summarized as follows: The first step reduces the noise in the image and enhances the robustness of edge detection; the second step highlights the edge information. Ambiguous edge points are filtered in the third step. Next, some edge points remaining from the third step are further filtered in the fourth step.

2.4 Hough transform detection

Hough transform was proposed by Paul Hough in 1962 and published as a patent in the United States [8]. It was first used to detect straight lines in images and later extended to detect circles, curves, and so on. Herein, we briefly introduce the basic principle of Hough transform line detection in the binary edge image after Canny edge detection.

The image is composed of discrete pixels, so a straight line that may exist in the image is also composed of a series of discrete points. Line detection by Hough transform involves a mapping relationship between (θ, r) and the line $y = kx + b$, which is one-to-one mapping. The principle of Hough transform is shown in Fig. 5.

The straight line in the figure is expressed as follows

$$y = -\frac{\cos\theta}{\sin\theta}\, x + \frac{r}{\sin\theta}, \tag{10}$$

what can be rewritten as

$$r = x\cos\theta + y\sin\theta\,. \tag{11}$$

The mapping relationship between (θ, r) and the straight line is explained below.

As shown in Fig. 5, for each straight line, a unique vertical line passes through the origin of the Cartesian coordinate system, and this vertical line is represented by (θ, r), where θ is the angle between the vertical line and the X axis and r is the length of the vertical line (the distance from the origin to the straight line). In case of a vertical line, the line is itself unique, because θ, r determines the point through which the line must pass and the slope of the line. That is, θ, r uniquely represents a line. The following describes how this relationship can be used to extract a line from an image.

The steps of the Hough transform algorithm are as follows:

(1) Determine the value range of r and θ, assuming that the image is located in the first quadrant of the rectangular coordinate system and the length is x and y, respectively. Then, the maximum value of r is $\sqrt{x^2 + y^2}$, so $r \in [0, \sqrt{x^2 + y^2}]$. Generally, $\theta \in [0, \pi/2]$; each degree is divided into an interval, so θ is divided into 90 intervals.

(2) The value ranges of r and θ are divided equally, and a two-dimensional accumulation array is established. Let the subscript of the two-dimensional array correspond to the values of r_i and θ_j.

(3) Hough transform is performed on all the edge points of the image, and r_i of each point after Hough transform at θ_j is calculated. If $(r_i, \theta_j$ corresponds to an array element, the value of the array element is increased by 1.

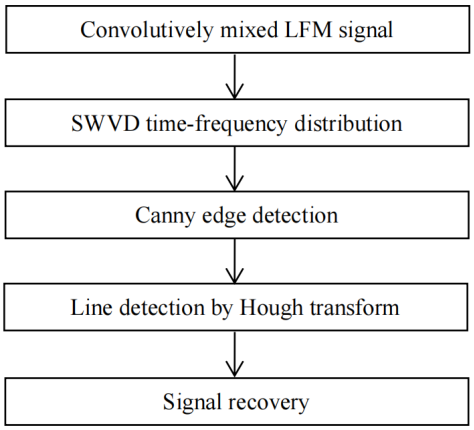

Fig. 6. Flow chart of the proposed algorithm

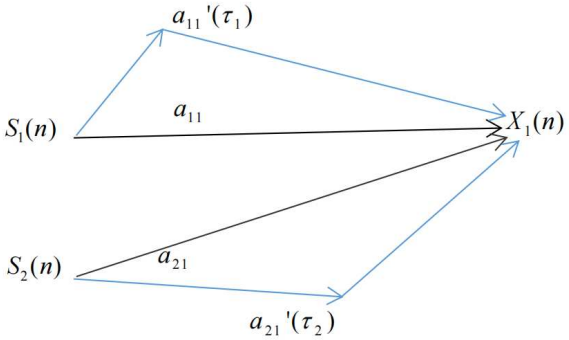

Fig. 7. Schematic diagram of a 2×1 single channel convolutively mixed model

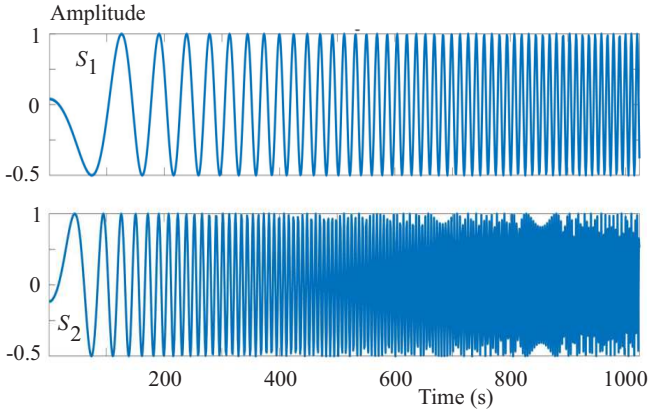

Fig. 8. Waveforms of source signal S_1 and S_2

(4) Comparing the values of array elements, the maximum values corresponding to (r_i, θ_j) are the parameters of the the linear equation corresponding to these collinear points.

Note that if the quantization of r and θ is too coarse, the linear parameters will not be accurate, and the amount of calculation will increase. Therefore, for r and θ quantization, both the quantization accuracy and the amount of calculation should be considered. In addition, Hough transform has strong anti-noise performance in detecting straight lines and can connect the broken edges.

2.5 Algorithm steps and flow chart

In this study, SWVD is used for the time-frequency analysis of the convolutively mixed LFM signal, Canny edge detection is used for the time-frequency analysis, Hough transform is used to detect and extract the line parameters in the edge, and finally the source signal is recovered using these parameters. The steps of the proposed algorithm are presented in Tab. 1.

Table 1. Algorithm steps and the main MATLAB code

Input: convolutively mixed LFM signal x Output: separated signal y

1: Suppose the length of χ data is N, draw its time-frequency distribution by WVD in color, and then convert it into a gray scale image.
[tfr_wvd,t,f] = tfrwv(χ,(1 : N), N); imagesc(t, f, tfr_wvd); axis xy;
rawimggray = rgb2gray(rawimg);
2: Canny edge detection for the gray scale image.
cannyimg = edge(double(rawimggray),'canny');
3: Extraction of line parameters axis_rho and axis_theta by Hough transform
[accum, axis_rho, axis_theta] = Hough(cannyimg);
4: Based on axis_theta and the coordinate range of the time-frequency distribution diagram, the new time-frequency diagram is redrawn; then, the LFM source signal is recovered.

Based on the above description, a more intuitive presentation of the steps is shown by the algorithm flow chart in Fig. 6.

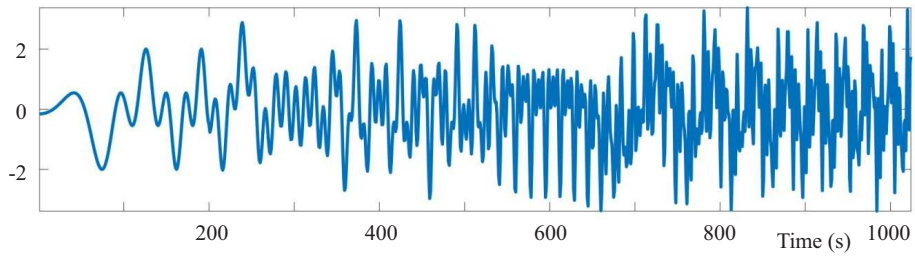

Fig. 9. Waveforms of mixed signal X_1

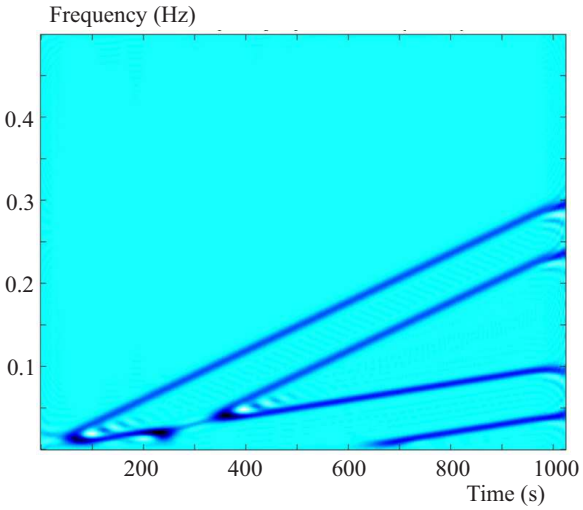

Fig. 10. SWVD time-frequency representation of $X_1(n)$

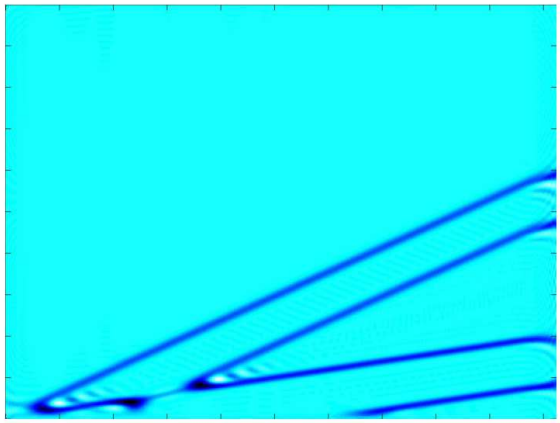

Fig. 11. Time-frequency image without coordinate axis

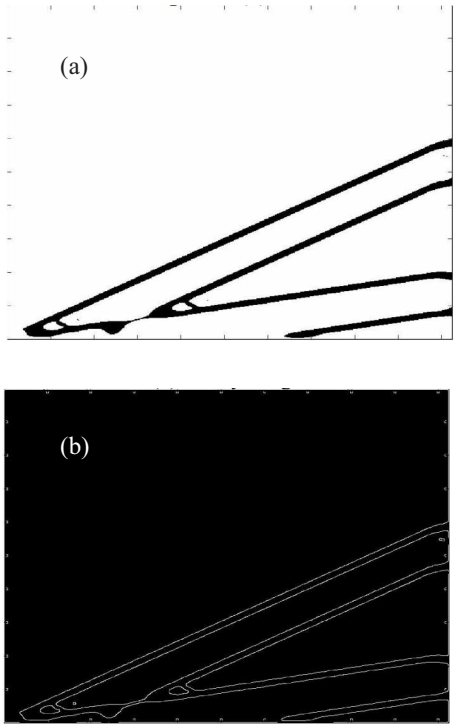

Fig. 12. Time-frequency image processing

3 Simulations and results

In this section, according to the method described in Section 2, the simulation experiment of single channel convolutively mixed blind source separation is carried out for LFM signals. For the convenience of describing the problem, the number of source signals is set to 2, the number of observation signals is now 1, and the number of paths is represented by the order of the finite impulse response (FIR) filter, which is set to 2. A 2×1 single channel convolutively mixed model is shown in Fig. 7.

To make the comparison as fair as possible, the experiments are carried out in the same hardware and software environment for each algorithm used in the comparison. The following simulations are repeated for many times, and finally the average correlation coefficient and average running time are obtained, which can reduce the randomness and improve the reliability of the results. All simulation experiments in this paper are based on the following computer software and hardware environment:

(1) Software: Windows 7 (64-bit version) + MATLAB 2017b

(2) Hardware: CPU Intel Core ^{TM} I7-2720qm processor 2.20GHz, RAM 16GB.

Simulation 1: The convolutively mixed LFM signal and its time-frequency distribution. To program easily, the function fmlin(N, Start_Freq, End_Freq) in MATLAB is used to generate an LFM waveform. In this function, N is the number of samples, Start_Freq is the initial frequency, End_Freq is the end frequency; they are normalized frequencies and can be obtained from the time-frequency distribution. The slope of the generated LFM signal G = End_Freq-Start_Freq. The signal amplitude of two LFM source signals is set to 1, the sampling frequency is 1024 Hz, and the number of sampling points is N = 1024. For the first LFM signal, Start_Freq = 0 and End_Freq = 0.1; for the second LFM signal, Start_Freq = 0 and End_Freq = 0.3. The time domain waveform of the two sources is shown in Fig. 8.

Here, for the sake of the clarity of the time-frequency analysis diagram, the effect of noise is not considered; that is, the mixed signal is subjected to denoising , assuming channel parameters $a_{11} = 0.8$, $a'_{11} = 0.6$, $a_{21} = 0.9$, $a'_{21} = 0.7$, delay $\tau_1 = 600$, and $\tau_2 = 200$. The expression of the single channel convolutively mixed signal $X_1(n)$ is

$$X_1(n) = 0.8S_1(n) + 0.6S_2(n-600) + 0.9S_2(n) + 0.7S_2(n-200)\,.$$

The time domain waveform of the convolutively mixed signal $X_1(n)$ is shown in Fig. 9.

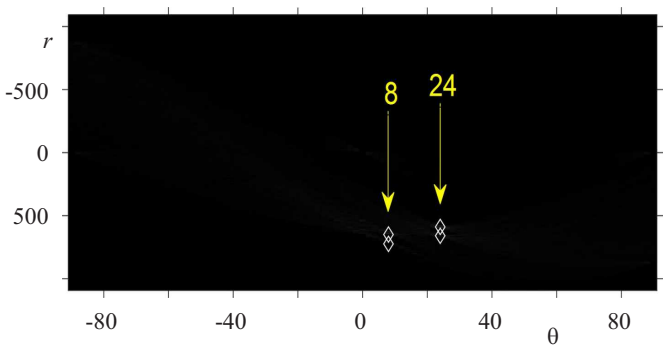

Fig. 13. Results of Hough transform

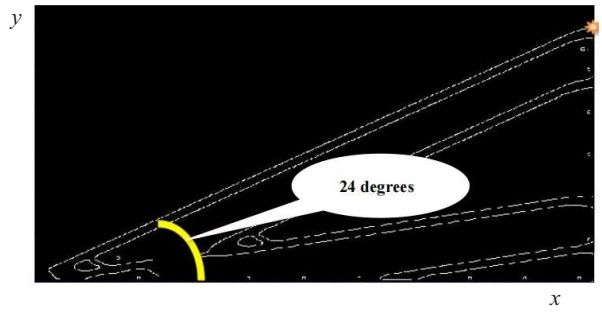

Fig. 14. First group of lines passing through the origin

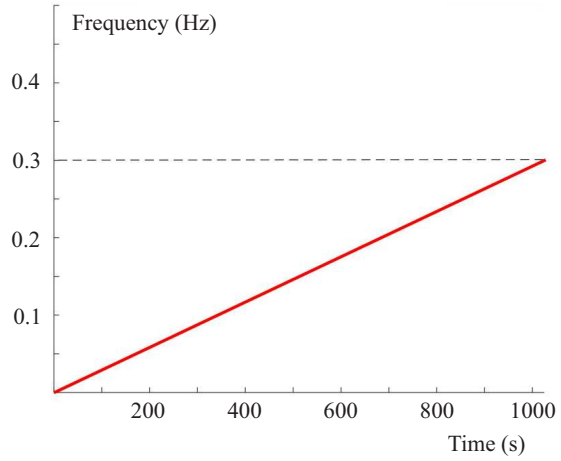

Fig. 15. First group of lines passing through the origin

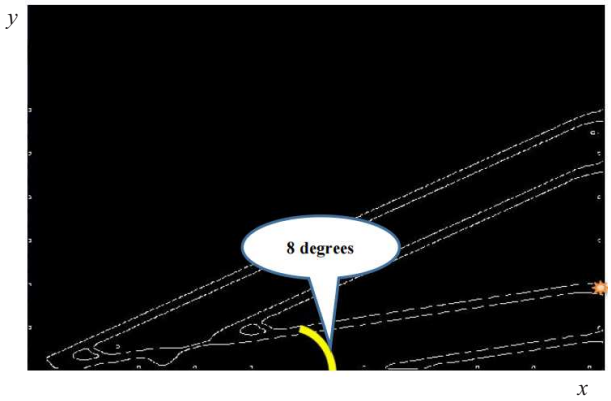

Fig. 16. Second group of lines passing through the origin

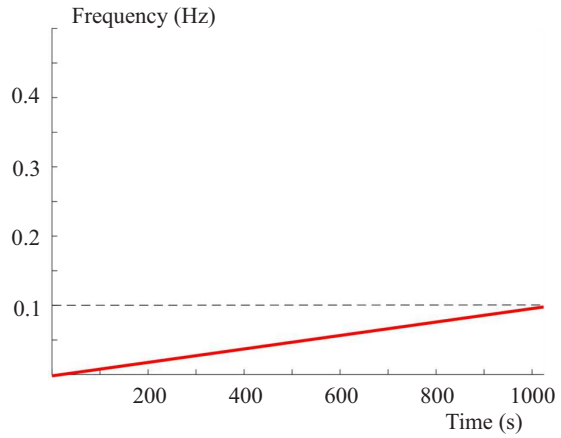

Fig. 17. Time-frequency diagram of the second recovered LFM signal

SWVD time-frequency representation of the convolutively mixed signal $X(n)$ is shown in Fig. 10.

The four lines in Fig. 10 correspond to four LFM signals in the mixed signal. There are two groups of parallel lines, each of which corresponds to the same LFM signal. The abscissa and ordinate represent time (in seconds) and frequency.

Simulation 2: Canny edge detection of time-frequency distribution For the post-processing, the coordinates displayed in the abscissa and ordinate of Fig. 10 are removed. This way, the above time-frequency distribution map is saved as a pure image in common format, such as BMP format, without the abscissa and ordinate, as shown in Fig. 11. Then, its size is automatically read (size: 875×656) in the program and recorded in the array.

Then, Fig. 11 is binarized and the result is shown in Fig. 12(a). Finally, Canny edge detection is performed and the result is shown in Fig. 12(b).

Simulation 3: Extraction of the number of lines and angles by Hough transform. Hough transform is performed on Fig. 12(b) and the result is shown in Fig. 13.

The four diamond white dots in Fig. 13 represent the four straight lines in the time-frequency diagram. The abscissa and ordinate represent θ and r, respectively. The figure shows that one group (two) of lines corresponds to an angle of 24 degrees, while the other group (two) of lines corresponds to an angle of 8 degrees.

Simulation 4: Source signal recovery By calculation, the slope of the first group of lines is $k_1 = \tan(24) = 0.45$. For Fig. 11 and Fig. 12(a),(b), the line with size 875×656 passing through the origin falls on the star in Fig. 14, denoted as Y. Because $\tan(24) = Y/875$, $Y = 390$ and $y/656 \sim 0.63$.. The first group of lines passing through the origin is shown in Fig. 14.

Referring to the coordinate range of the time-frequency diagram, the time range is 0–1024s and the frequency

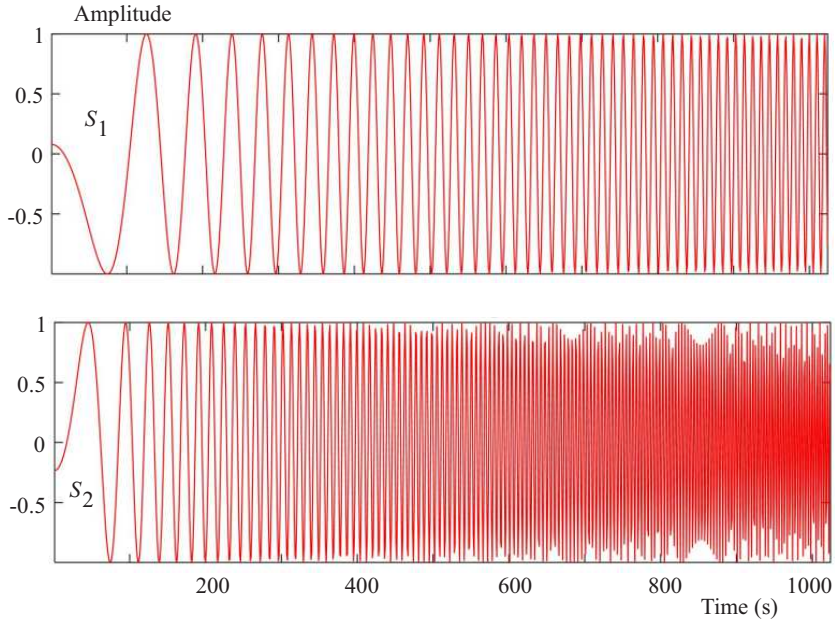

Fig. 18. Waveforms of two recovered LFM signals

range is $0-0.5$ Hz. It is easy to deduce the time-frequency diagram corresponding to this line, as shown in Fig. 15.

Similarly, the slope of the second group of lines is $k_2 = \tan(8) = 0.14$. For Fig. 11 and Fig. 12(a), (b), the line with size 875×656 passing through the origin falls on the star in Fig. 14, denoted as Y. Because $tan(8) = Y/875$, $Y = 123$ and $Y/625 \sim 0.2$. The second group of lines passing through the origin is shown in Fig. 16.

Referring to the coordinate range of the time-frequency diagram, the time range is 0–1024 s and the frequency range is 0000.5 Hz. It is easy to deduce the time-frequency diagram corresponding to this line, as shown in Fig. 17.

According to Fig. 15 and Fig. 17, the initial frequency is 0 and the end frequency is 0.3 and 0.1 (unit: Hz) respectively. Therefore, it is easy to obtain the time domain diagram of two LFM signals without delay (the line on the time-frequency diagram passes through the origin) as shown in Fig. 18.

After calculating, the correlation coefficient of the recovered signal and the source signal in Fig. 18 is 0.9999, which shows that the scheme achieves the effect of SCBSS.

Simulation 5: To further prove the feasibility of the algorithm, we choose another popular unsupervised SCBSS algorithm, Itakura-Saito nonnegative matrix two-dimensional factorization (IS-NMF2D) [12], to compare with our proposed algorithm. For as fair comparison as possible, the experiment is carried out in the same hardware and software environment for both algorithms. The average correlation coefficient between the separated signal and the source signal and the average running time of all programs (in seconds) for both algorithms are obtained [14, 15]. The separation performance comparison results of the two algorithms are shown in Tab. 2.

Table 2. Comparison of separation performance of the proposed algorithm and the IS-NMF2D algorithm

Algorithm	Average correlation coefficient	Average running time (s)
Proposed algorithm	0.9999	1
IS-NMF2D algorithm [12]	0.9600	14

Table 2 indicates that the proposed algorithm has better separation performance (separation accuracy) and calculation speed (bold text) in SCBSS of convolutively mixed LFM signals.

4 Conclusions

To address the single channel underdetermined blind source separation problem in a convolutively mixed signal model, this study adopted LFM signals as an example and proposed an SCBSS algorithm for convolutively mixed LFM signals based on SWVD time-frequency analysis, Canny edge detection, and Hough transform detection. On the premise of studying the time-frequency characteristics of the convolutively mixed LFM signals, the time-frequency analysis results (SWVD time-frequency analysis diagram) were obtained as images and the signal feature extraction (Hough line detection) was carried out using image processing (Canny edge detection). Finally, the source signal was recovered. The simulation results showed that the scheme achieves performance in single channel detection and extraction of convolutively mixed LFM signals.

Acknowledgements

This work was partially supported by the Start-up Fund for Talent Introduction and Scientific Research of Suqian University, No.106-CK0004296,106-CK00042/020, Jiangsu Agricultural Science and Technology Innovation Fund, No.CX(22)3109, and National Natural Science Foundation of China, No.62001183.

References

[1] H. Zhaoshui, X. Shengli, and F. Yuli, "Sparse representation and blind source separation of ill-posed mixtures", *Science in China Series F: Information Sciences*, vol. 49, no. 5, pp. 639–652, https://doi.org/10.1007/S11432-006-2020-8, 2006.

[2] A. Ozerov, P. Philippe, R. Gribonval, and F. Bimbot, "Choice and adaptation of statistical models for single channel singing voice separation", *Traitement du Signal*, vol. 24, no. 3, pp. 211–224, 2007.

[3] R. Tao, N. Zhang, and Y. Wang, "Analysing and compensating the effects of range and Doppler frequency migrations in linear frequency modulation pulse compression radar", *IET Radar Sonar and Navigation*, vol. 5, no. 1, pp. 12–22, https: //doi.org/10.1049/IET-RSN.2009.0265, 2011.

[4] B. Reynders and S. Pollin, "Chirp spread spectrum as a modulation technique for long range communication", *Symposium on Communications and Vehicular Technologies*, https://doi.org /10.1109/SCVT. 2016.7797659, 2016.

[5] G. Ben, X. Zheng, Y. Wang, N. Zhang, and X. Zhang, "A Local Search Maximum Likelihood Parameter Estimator of Chirp Signal", *Applied Sciences*, vol. 11, no. 2, pp. 673, https://doi.org/ 10.3390/APP11020673, 2021.

[6] W. Gongjian, *Research on dynamic gesture recognition algorithm based on smoothed pseudo Wigner-Ville distribution*, PhD thessis, Beijing University of Posts and Telecommunications, Beijing, China, 2016.

[7] J. Canny, J, "A Computational Approach to Edge Detection", *IEEE Transactions on Pattern Analysis and Machine Intelligence*, vol. 8, no. 6, pp. 679-698, https://doi.org/10.1109/TPAMI.1986.4767851, 1986.

[8] P. V. C. Hough, "Method and means for recognizing complex patterns", *US Patent 3,069,645*, 1960.

[9] L. Durak and O. Arikan, "Short-time Fourier transform: two fundamental properties and an optimal implementation", *IEEE Transactions on Signal Processing*, vol. 51, no. 5, pp. 1231–1242, https://doi.org/10.1109/TSP.2003.810293, 2003.

[10] L. Xiumei and Y. Guoqing, "Performance comparisons among time-frequency representations", *Computer Simulation*, vol. 32, no. 03, pp. 220–224, 2015.

[11] S. Peiqing, *Research on methods and implement of radar signal digital channlized reconnaissance based on STFT*, PhD thessis. University of Electronic Science and Technology of China, Chengdu, China.

[12] B. Gao, W. L. Woo, S. S. Dlay, "Unsupervised Single-Channel Separation of Nonstationary Signals Using Gammatone Filterbank and Itakura - Saito Nonnegative Matrix Two-Dimensional Factorizations", *IEEE Transactions on Circuits and Systems I-Regular Papers*, vol. 60, no. 3, pp. 662–675, https://doi.org/10.1109/TCSI.2012.2215735, 2013.

[13] E. P. Wigner, "On the quantum correction for thermodynamic equilibrium", *Physical Review*, vol. 40, no. 5, pp. 749–759, https://doi.org/10.1103/PHYSREV.40.749, 1932.

[14] P. Xu, Y. Jia, Z. Wang, and M. Jiang, "Underdetermined Blind Source Separation for Sparse Signals based on the Law of Large Numbers and Minimum Intersection Angle Rule", *Circuits Systems and Signal Processing*, vol. 39, no. 5, pp. 2442-2458, https://doi.org/10.1007/S00034-019-01263-2, 2020.

[15] Y. Jia and P. Xu, "Convolutive Blind Source Separation for Communication Signals Based on the Sliding Z-Transform", *IEEE Access*, no. 8, pp. 41213-41219, https://doi.org/10.1109/ACCESS.2020.2976700, 2020.

Received 31 October 2022

Pengfei Xu PhD, lecturer, graduated from Hohai university, majoring in signal processing and machine learning, now working in the school of information engineering of Suqian university. Yinjie Jia, PhD, lecturer, graduated from Hohai university, majoring in signal processing and machine learning, now working in the school of information engineering of Suqian university.

Xinnian Guo PhD, associate professor, graduated from Nanjing university, majoring in adaptive signal processing and machine learning, now working in the school of information engineering of Suqian university.